# Thermal Severing. The Cutting of Brittle Materials by Thermally Induced Fracture

J. N. DEKKER and M. H. ZONNEVELD
*Philips Research Laboratories, Eindhoven, The Netherlands*

***Abstract:*** *Traditional methods of cutting brittle materials have the disadvantage that a rough cut edge results, so that in many cases subsequent grinding is necessary. Another disadvantage is that small chips are formed which can adhere to the surface. For some products this can be disastrous. The alternative presented in this paper is thermal severing, a method where a relatively slow running crack is induced and controlled by thermal stresses. To obtain a smooth crack surface, a low fracture speed, or in fact a low energy release rate, is essential. With the process, very smooth edges can be produced in a simple manner, without chips and dust particles being formed. Two principles of thermal severing will be treated: severing with a moving hot-spot (e.g. a $CO_2$-laser) and severing with a stationary linear heat source. For both methods, experiments and finite element calculations will be described. Some special attention is paid to the use of the singular element developed by Morris Stern.*

***Keywords:*** *Fracture, Cutting, Severing, Brittle-Materials, Glass, Thermal-Stress, Laser, Finite-Element-Method, Controlled-Fracture, Crack-Path.*

## INTRODUCTION

Traditional methods of cutting brittle materials are, for example, scoring and bending (used by the glazier cutting window panes), sawing (e.g. ferrites and silicon) and thermal cracking-off (often used for cutting glass tubes). Less traditional is the use of a laser for the cutting by evaporation. The word evaporation is emphasized to make a distinction from the later discussed thermal severing with a $CO_2$-laser. Figure 1 illustrates three cut edges of glass plates, the upper made by sawing, the lower by scoring and bending. Those two edges indicate rough edge surfaces so that, for some applications, a subsequent grinding operation will be necessary. Furthermore, these edges have the disadvantage of the creation of splinters and dust particles, which can adhere to the surface. For some products this can be disastrous.

The alternative we have investigated is thermal severing. This is a cutting method in which constructive use is made of fracture; a crack is induced and controlled by thermal stresses. In Fig. 1 the cut edge in the middle has resulted from thermal severing. A vast improvement in surface quality is evident. The cutting of glass by thermal stresses has been known for centuries. Sometimes, a hot steel rod was used to cut the glass parts of leaded windows. The previously mentioned thermal cracking-off is another example of thermal severing, which has been used in glass workshops and industry for many years. However, an impor-

tant difference between these existing methods and the methods of thermal severing considered in this paper is the controlled crack velocity of the latter.

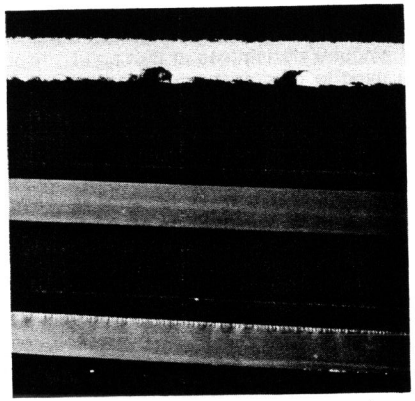

*Fig. 1: Cut-edges made by sawing, thermal severing and scoring & bending.*

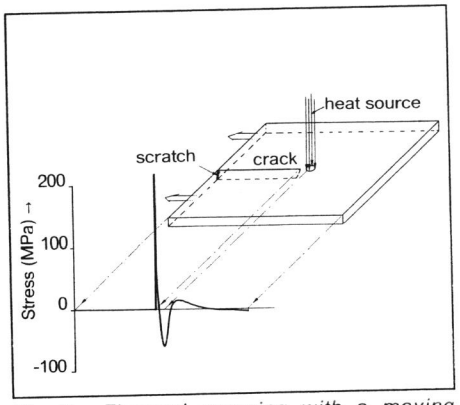


*Fig. 2: Thermal severing with a moving hot-spot.*

We have investigated two methods of thermal severing. Firstly, severing with a moving spot-shaped heat source. The principle involved is illustrated in Fig. 2. On the edge of a plate a scratch is made, a heat source is moved over the scratch whereupon a crack pops in from the scratch. If the heat source is moved further over the plate, the crack tip follows at a small distance. How this method operates can be seen from the stress component normal to the crack plane. The material in the vicinity of the heat source will expand more than the surrounding material; this causes a compressive stress surrounded by tensile stress. Now the tensile stress between the crack tip and the heat source will cause the crack to proceed. It can also be seen that the crack can never run through the heated zone, because of the compressive stress.

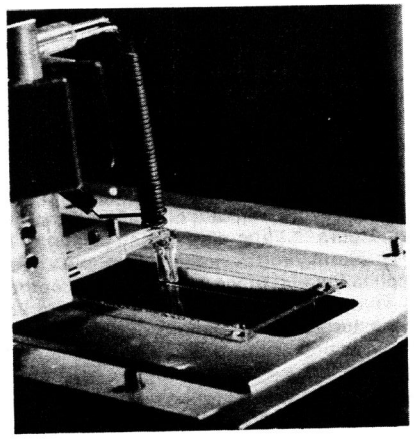

*Fig. 3: Thermal severing with impinging air.*

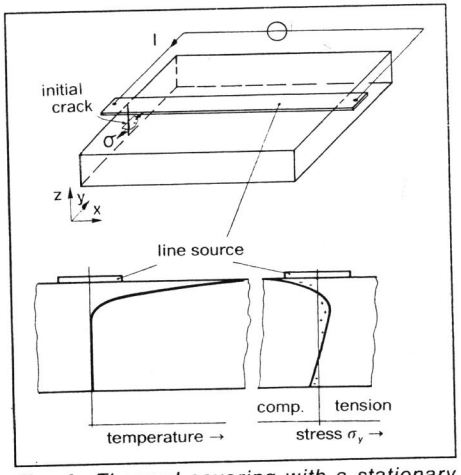


*Fig. 4: Thermal severing with a stationary linear heat source.*

In other literature, several implementations can be found: heating with hot air (Stahn *et al.*, 1980), heating with an out of focus laser beam (Lumley, 1969 and Grove *et al.*, 1971) and



dielectric heating (Lins, 1965). We have built experimental set-ups according to the first two implementations. The first after Stahn *et al.* (1980) is illustrated in Fig. 3. On the edge of the glass plate a scratch is made. From two quartz tubes air is flowing; the anterior is heated to ca. 300 °C. After moving the impinging air jets over the glass plate, a crack eminates from the initial crack. The crack tip follows at a short distance behind the hot jet. The cold air jet is added to increase the thermal gradients; this is not, however, strictly necessary.

The second method we have investigated is thermal severing with a stationary linear heat source, as illustrated in Fig. 4. On the edge of the plate again an initial crack is made; in this instance however it must be made with a specific, well-defined depth (by controlling the scratch force). Next, a linear heat source is exposed to the surface. After heating for a short time, a crack will pop in from the initial crack and will run with a relatively high speed through the plate. The way this method works depends to a great extend on the thickness of the sheet material. For relatively thick material the temperature gradients in the thickness direction cause the severing. Figure 4 shows that, as a result of the relatively high temperature, there will be a compressive stress in the material near the upper surface, a tensile stress in the middle part of the plate and, to get bending moment equilibrium, a compressive stress at the lower surface. The tensile stress in the middle causes a crack to be induced. For relatively thin sheets the stresses caused by in-plane thermal gradients are of importance as well; this will be shown in the next chapter.

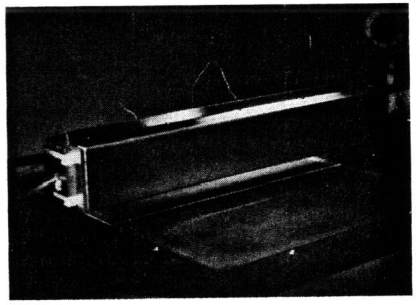

*Fig. 5: Thermal severing with a contact conduction line source.*

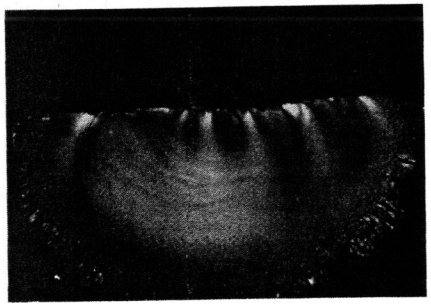

*Fig. 6: A glass fracture surface (courtesy Freimann, 1980)*

In other literature several inplementations can be found with various ways of heating: contact conduction (Stahn and Döll, 1978) radiation and convection (Oelke, 1969) and dielectric heating (Pilkington Br. Ltd., 1968). (For the latter, the driving stresses are always induced by the in-plane thermal gradients, independent of the sheet thickness). In Fig. 5 our experimental set-up with contact conduction heat source is illustrated. An electrically heated bar is brought into contact with the plate. The contact width is ca. 1 mm.

A characteristic common to both methods is that the energy release rate can be controlled. That this is essential can be seen from Fig. 6 (Freimann, 1980). In this illustration a typical glass fracture surface is depicted. A crack is originated from the flaw and has run accelerating in radial direction. Several regions can be seen on the fracture surface. Surrounding the initial crack a smooth, shiny region, known as the fracture mirror, can be recognized. The next two regions, known as mist and hackle zone, are generally to be thought of as representing the initiation and limited propagation of secondary cracks (microscopic crack branching). Finally, macroscopic crack branching occurs. The crack branching phenomena are formed due to the excess of kinetic energy, gained from a surplus of strain energy. Hence, to achieve a smooth surface the energy release rate has to be controlled so as to prevent accumulation of kinetic energy. Then the crack tip speed will be relatively low. It is clear that in the moving-hot-spot method the crack tip velocity is equal to the velocity of the moving spot, and it will be shown that the energy release rate at the tip is equal to the critical energy release rate. For the stationary-line-source method it is less clear; it will be shown that the depth of the initial crack stipulates a controlled fracture.

## FINITE ELEMENT MODELLING AND EXPERIMENTS

### The Moving Hot-Spot Method

For the modelling of the moving-spot method we have considered the implementation with a $CO_2$ -laser which radiates on glass, so that all energy is absorbed in a thin layer near the surface. The calculations have been performed with the finite element package SEPRAN (Segal, 1984). Firstly, a three-dimensional temperature calculation is performed, the result of which is illustrated in Fig. 7. The temperature distribution is determined by the Peclet number with respect to the thickness: $Pe_t = \rho cvt/\lambda$ where $\rho$ is the density, $c$ the heat capacitance, $v$ the velocity of the spot, $t$ the thickness of the plate and $\lambda$ the heat conduction coefficient. For small values of the Peclet number ($Pe_t < ca.15$), the gradients in thickness direction are small. Then a two-dimensional calculation is sufficient; see Fig. 8a.


***Fig. 7:*** *3D-temperature distribution. The front edge is the symmetry plane.*

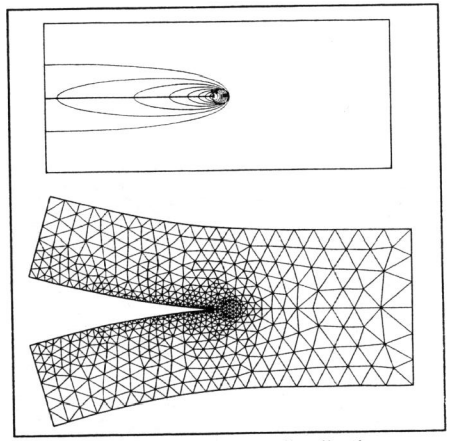

***Fig. 8:*** ***a.*** *2D-temperature distribution.* ***b.*** *Deformed geometry.*

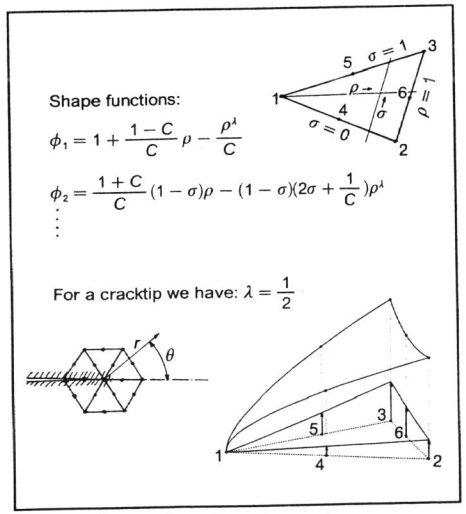


***Fig. 9:*** *Stern singular element.*

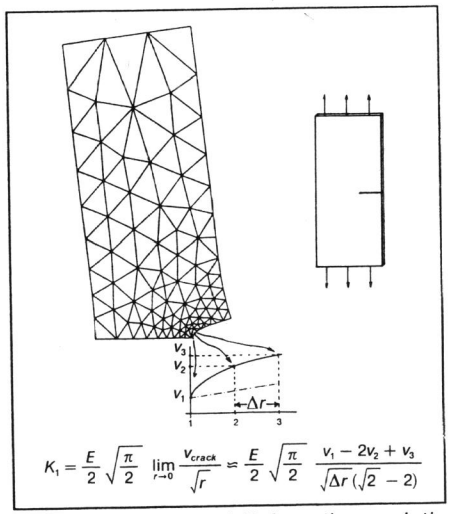


***Fig. 10:*** *Derivation of $K_1$ from the crack tip displacement field.*



From this temperature distribution the deformation field is derived with plane stress elements; see Fig. 8b. The crack is opened by the thermal expansion of the material along the crack; the crack opening is in the order of tenths of millimetres (depending on the length of the crack). The stress component normal to the crack plane can be seen in Fig. 2. Because the material was modelled as a linear elastic continuum, the stress at the crack tip is infinitely high, or better, the displacement field has singular derivatives at that point. Therefore, linear elastic fracture mechanics has been used to predict the crack progress. For modelling the singular derivative displacement field in the vicinity of the crack tip, we implemented the singular element developed by Stern (1979) in the SEPRAN package. This element differs from other more often used singular elements (such as the quarter noded isoparametric quadrilateral element) in the linear part of the shape functions; see Fig. 9. Due to the linear part it is possible to describe a constant temperature expansion without introducing a K-value. The singular elements are put around the crack tip and the rest of the plate is filled with ordinary polynomial elements. The Stern element can be made to conform with polynomial elements of any order. Figure 10 indicates how the $K_1$-value was deduced from the crack tip displacement field. In the asymmetrical case the difference in displacement between upper and lower crack face has been used. We also performed a J-integral calculation with the area integral correction term for the presence of thermal stresses, derived by Wilson and Yu (1979). However, probably due to the large thermal gradients, the results were less accurate than those directly derived from the crack tip displacement field.

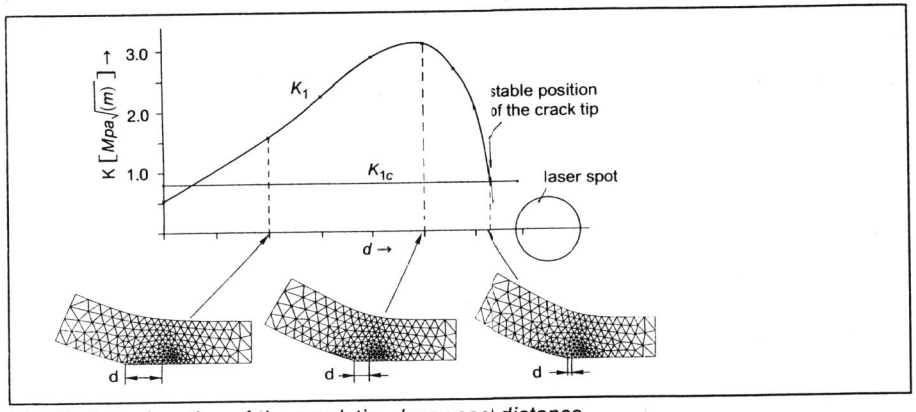


***Fig. 11:*** *$K_1$ as function of the crack tip - laser spot distance.*

To model thermal severing with a moving hot-spot, $K_1$ is calculated for several distances between the crack tip and the laser spot. Figure 11 illustrates the result of this action. $K_{1c}$ is also shown in this figure. The equilibrium position of the crack tip with respect to the moving laser spot is given by the anterior intersection point of $K_{1c}$ and $K_1$-curve. Then, the energy release rate $G$ is equal to the critical energy release rate $G_c$. The equilibrium position thus calculated, has also been verified experimentally. Figure 12 illustrates the experimental set-up. The tube in the upper part of the photograph is the end of the beam delivery system. The laser is radiating just in front of the crack tip. The spot is not visible because of the high wavelength of 10.6 $\mu m$. With a video camera, which views from underneath through the glass, the picture illustrated in Fig. 13 is obtained. At the left the rear of the spot is made visible in white. The stripe above the millimetre scale is the crack. The crack tip runs approximately 1.5 mm behind the laser spot. The thus measured value agrees with the calculated value within approximately 0.3 mm.

An example of parameter variation is given in Fig. 14. Here, the $K_1$-curve for three velocities of the laser spot is given. The laser power was adapted to the velocity such that the maximum temperature was constant. The intersection point of the $K_1$-curve with $K_{1c}$ shifts backwards with increasing velocity. If the velocity is increased further, at some speed the

$K_1$-curve lies entirely below $K_{1c}$. The crack tip then no longer follows the laser spot. Another parameter which turned out to have a strong influence was the width of the plate. In Fig. 15 the $K_1$-curves for two different widths are given. The equilibrium point shifts backwards with increasing width. Furthermore, the $K_1$ becomes lower, indicating that cutting a large plate is more difficult than cutting a slender plate. At a certain width $K_1$ becomes lower than $K_{1c}$, and cutting is no longer possible. However, for many materials an adjustment of the process parameters can be found that facilitates severing of plates with an infinite width.

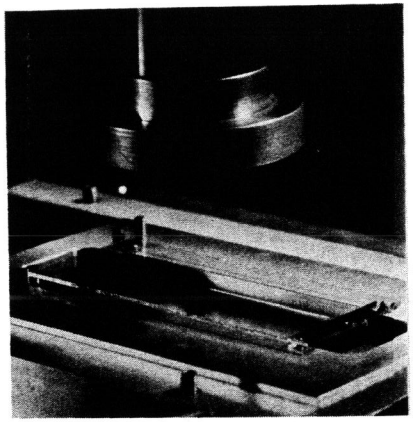

*Fig. 12: Thermal severing with a $CO_2$-laser.*

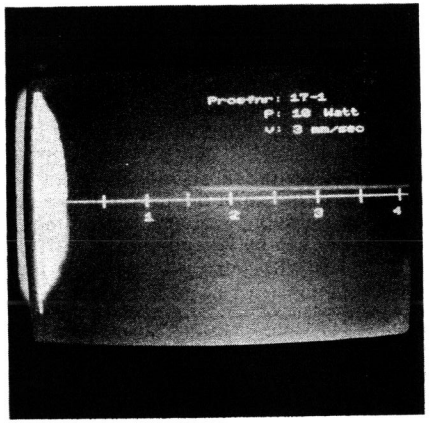


*Fig. 13: Measuring the crack tip position.*

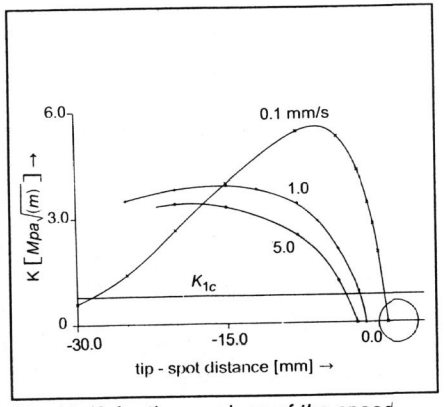


*Fig. 14: $K_1$ for three values of the speed.*

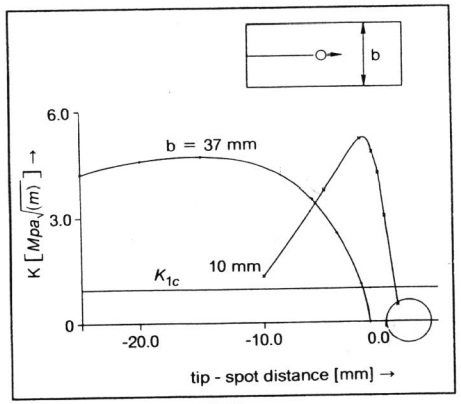


*Fig. 15: $K_1$ for two widths.*

Thus far the modelling was only valid for a cut made symmetrically in the plate. If, however, a cut is made near the edge of the plate or if contours are made, symmetry no longer exists. The effect that can be observed then is that the crack no longer follows the track of the laser spot, but shows a small lateral deviation as can be seen in Fig. 16c. This deviation is not due to thermal asymmetry, but due to the difference in in-plane stiffness of the parts of the plate on both sides of the crack. Figure 16a illustrates the temperature distribution in an asymmetrical severed plate. It shows hardly any asymmetry. Because the material near the crack is warmer than the material away from the crack, the parts of the plate on both sides of the crack will bend outwards. However, the slender part will bend more than the broad one, as is illustrated in Fig. 16b. This causes a discontinuity in $\sigma_x$ on a cross-section perpendicular to the crack at a small distance behind the crack tip (see Fig. 16b). Due to this, a shear load on the crack plane will be induced, causing $K_2$ to be nonzero.



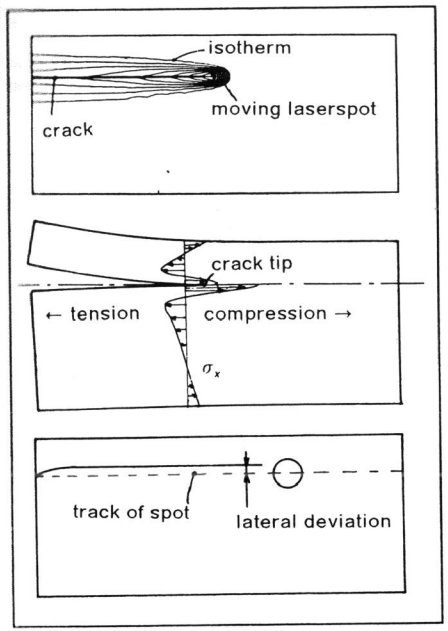


*Fig. 16: Asymmetrical severing.*
*a. Temperature distribution.*
*b. Deformed geometry and $\sigma_x$*
*c. Lateral deviation.*

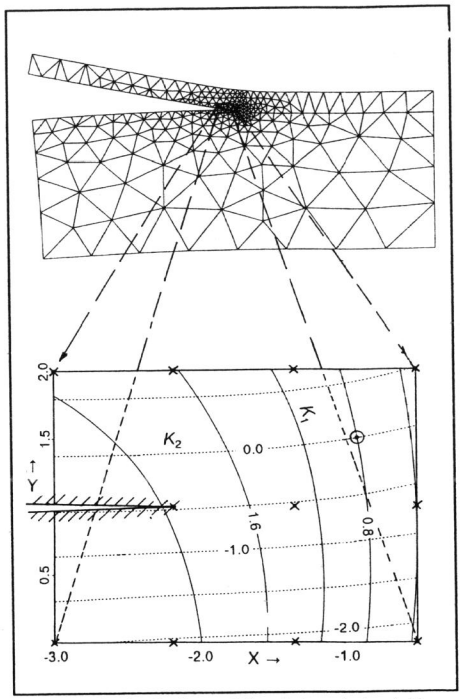


*Fig. 17: Calculation of the lateral deviation.*

To calculate the lateral deviation, we make use of the principle of local symmetry (Cotterell and Rice, 1980; Amestoy and Leblond, 1986) that states, that a running crack will search its way such that $K_2$ is zero. In other words, if there is a shear load on the material at the crack tip, the crack will change its direction. The way this criterion is used to calculate the lateral deviation is illustrated in Fig. 17. On a small area behind the laser spot, the position of the crack tip is varied. The various positions are denoted by the small crosses in the lower part of the figure. In each of these positions $K_1$ and $K_2$ are calculated. $K_2$ is derived from the x-component of the nodal displacement at the crack tip. We also applied a $J_2$-integral calculation, with both the Wilson and Yu (1979) thermal gradients correction and the method developed by Eishen (1987) for evaluating the singular crack face integral. However, again the most accurate results were obtained with derivation of $K_2$ from the displacement field.

Next, the contour plot illustrated in the lower part of Fig. 17 is generated; the solid lines show $K_1$, the dashed lines $K_2$. Now the equilibrium position of the crack tip with respect to the moving laser spot will be found from the intersection point of the $K_2 = 0$ and the $K_1 = K_{1c}$ line, for which in this instance 0.8 $MPa\sqrt{m}$, the value for glass is taken. In this example the lateral deviation is of the order of 1 mm. We have verified this with experiments: the calculated value was in agreement within 0.1 mm. The lateral deviation can be made smaller by optimization of the process parameters.

Discussing the influence of all other process parameters would be beyond the scope of this paper. Therefore only the most important parameters will be mentioned. Of the material properties the thermal diffusivity, thermal expansion, modulus of elasticity, melting or glass transition temperature and fracture resistance are of importance. The required values cannot be given; the properties are interchangeable. Of the process parameters the velocity, diameter and power of the spot are the most important. We have already shown that the geometry of the product has a strong influence.

## The Stationary Line-Source Method

With the line-source method we are especially interested in the way the energy release rate can be controlled. We found that it can be controlled by controlling the depth of the initial crack on the edge of the plate. In this paper only a qualitative analysis will be presented. A more quantitative treatment will be published elsewhere.

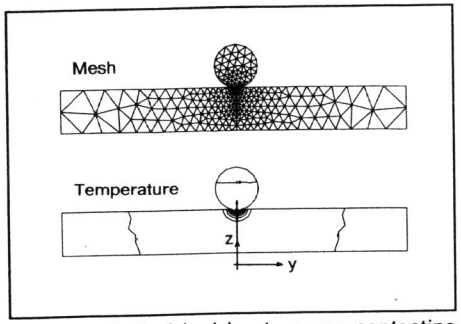


***Fig. 18:*** *Cylindrical heat source contacting a glass plate.*

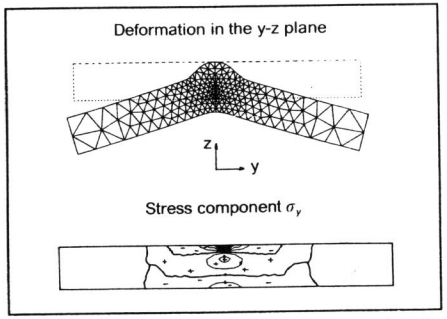


***Fig. 19:*** *Deformation and stress $\sigma_y$ due to thickness gradients.*

We start again with a temperature calculation; for the heat source a cylindrical bar is taken, which is maintained at a specific temperature by electrical heating. It is brought in contact with the plate and after a short time a temperature distribution will occur as shown in Fig. 18. Large thermal gradients arise near the surface. Firstly, the plate is assumed to be infinitely long in the direction of the heat source. Then with generalized plane strain elements the deformation and stresses are calculated. In Fig. 19 the deformation in the plane normal to the crack plane and the stress component in the y-direction are given. Near the point where the heat source contacts the surface a compressive stress will arise. Furthermore, a tensile stress in the middle and again a compressive stress at the lower surface will be induced. The maximum stress increases with time.

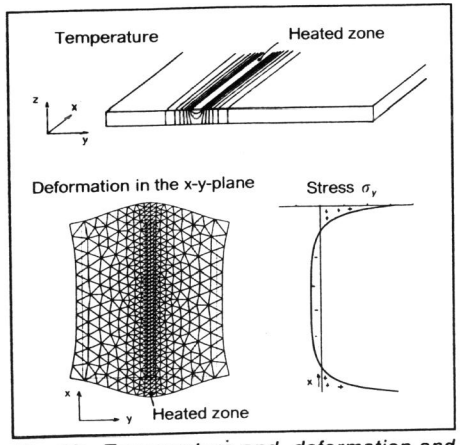


***Fig. 20:*** *Temperature and, deformation and stress due to in-plane thermal gradients.*

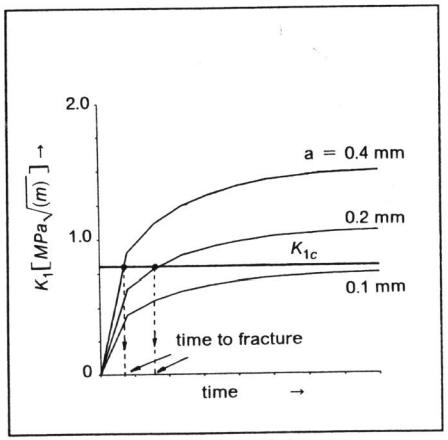


***Fig. 21:*** *$K_1$ as a function of time.*

In reality however, the plate has a finite width, which means that stresses normal to the crack plane are induced by the thermal gradients in the plane of the plate as well. For thin sheets they are even larger than the stresses caused by gradients in the thickness direction



and appeared to be the main driving force for severing. Figure 20 shows a three-dimensional sketch of the temperature, for an elapsed time several seconds longer than in Fig. 19. Because the material in the vicinity of the line source is warmer than the material away from the source, there will be a difference in thermal expansion. The difference in expansion in the longitudinal direction (x-direction) causes a tensile stress at both ends of the line source and a compressive stress in the middle (see Fig. 20). The maximum stress increases with time and after heating for a short time, the crack will start. Then the tensile stress region moves along with the tip. Which of the two mechanisms dominates depends to a great extend on the thermal properties of the material and the dimensions of the plate. However, both have in common that the maximum stress increases with time, although the stress rates differ. (For longer times the stress will decrease again.) The stress intensity factor at the initial crack is now estimated from $K_1 = 1.12\,\sigma_{max}\sqrt{\pi a}$ , the formula for small edge cracks. In Fig. 21 this is illustrated for three values of the crack depth $a$. It can be observed that the moment the crack starts is determined by the depth of the initial crack. For a small initial crack $K_1$ will never become large enough to start a crack.

The amount of elastic energy stored in the plate also increases with time. Therefore, the sooner the crack starts (i.e. the deeper the initial crack has to be made), the lower the energy release rate $G$ at the tip of the running crack will be. In the introduction it has already been explained on the basis of Fig. 6 that, in the instance of a low energy release rate, crack branching phenomena, causing a rough surface and splinters, do not occur. Hence, a smooth fracture surface is obtained if the initial crack is made deep.

There is still much doubt about the level of energy release rate at which crack branching phenomena occur. Broek (1986) describes several mechanisms of crack branching which already occur at values of $G$ in the order of 1.5 $G_c$. Freiman (1980) gives a survey of fracture mirror data of several authors, which all lead to a criterion $G >$ ca. $4G_c$ for microscopic crack branching. However, that the exact value is not very important is illustrated by Fig. 22. Depicted here is the relation between the elastic energy release rate and the crack tip speed, experimentally determined by Kerkhof en Richter (1969). If one makes $G$ for instance only 1.1 $G_c$ , the fracture velocity will still be of the order of 100 m/s. Then in practice, the time required to make the cut is almost entirely determined by the heating time.

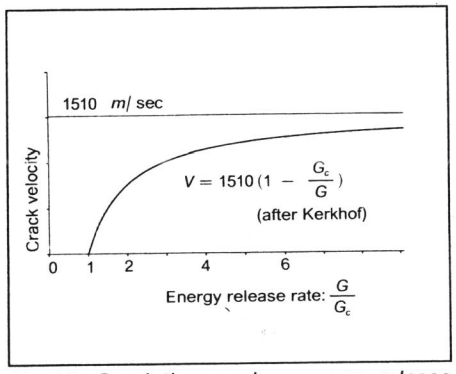


***Fig. 22:*** *Crack tip speed vs. energy release rate after Kerkhof and Richter (1969).*

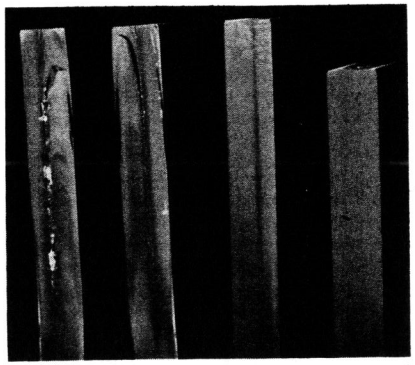

***Fig. 23:*** *Cut edge quality for increasing initial crack depth.*

We have also verified experimentally the influence of the initial crack on the fracture surface quality. Figure 23 shows a photograph of four cut edges of 19 mm thick glass plates. Each of them, before severing, was provided with a scratch, made with an increasing scratch force. It can be observed that, for a sufficient scratch force, i.e. a sufficient initial crack depth, an extremely smooth and perfect fracture surface is achieved.

## SOME FEATURES OF THERMAL SEVERING

With symmetrical thermal severing a straightness within 10 $\mu m$ can be reached. Even better results can be achieved if special attention is paid to the way the plate is supported. Roughness values of the order of 10 nm are feasible in glass. Thermal severing offers the possibility of contour cutting, although there are some restrictions on the form. A fine property of a cut made by thermal severing is that both halves fit on each other perfectly, since there is no material removed or any plastically deformed. Another feature of thermal severing with a moving hot-spot is that a corrugated surface can be cut whilst the heat source is moving in a straight line. At a specific adjustment of velocity and power, the crack appears to move in a stable oscillating manner behind the linearly moving heat source. The result of this is shown in Fig. 24. Both properties were used te cut ferrite rings for CRT deflection coils. These are divided into halves to be wound, after which both halves have to be reassembled perfectly fitting, to minimize magnetic reluctance. To make a simple assembly possible, a corrugated cut is made; see Fig. 25.

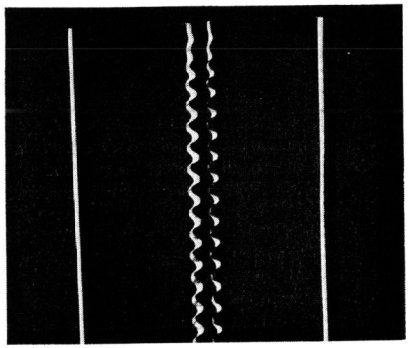

***Fig. 24:*** *Corrugated edge made by severing with a moving impinging hot air jet.*

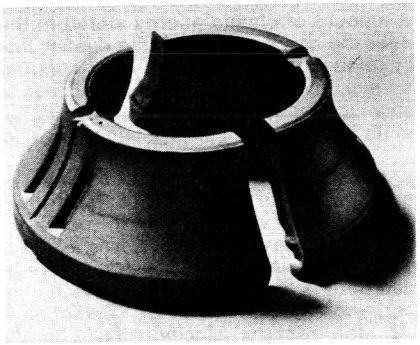

***Fig. 25:*** *Yokerings for deflection coils divided with partially corrugated cuts.*

## REFERENCES


Amestoy M. and J.B. Leblond(1986). Curvelinear cracks in planar situations. In: *Eur. Conf. Frac. 6*, Amsterdam, pp:1377-1401.

Broek D. (1986). *Elementary engineering fracture mechanics*. Mart. Nijhoff, Dordrecht.

Cotterell B. and J.R. Rice (1980). Slightly curved or kinked cracks. *Int. J. of Fracture*, 16, 155-169.

Eishen J.W. (1987). An improved method for computing the $J_2$ -integral. *Eng. Fract. Mech* 26, 691-700.

Freimann S.W. (1980), Fracture mechanics of glass, In: *Glass: science and technology* (D.R.Uhlmann and N.J.Kreidl, ed.), vol. 5, Ac. Press, New York.

Grove F.J., D.C. Wright and F.M. Hamer (1971). Improvements in or relating to the cutting of glass. *U.K. Patent 1246481*, applicant: Pilkington Brothers Ltd, GB.

Kerkhof F. and H. Richter (1969). *ICF2*, Brighton, 401-412.

Lins R.G. (1965). Cutting solid dielectric materials with radio-frequency energy. *US patent: 3183339*

Lumley R.M. (1969). Controlled separation of brittle materials using a laser. *Ceramics Bulletin*, 48, 850-854, (Am. Cer. Soc.)

Oelke W. (1969). Apparatus for cutting glass plates. *US Patent 3587956*.

Pilkington Brothers Ltd. (1968). Verfahren und Vorrichtungen zum Schneiden von Glass. *Offenlegungsschrift 1916076*, inventor unknown.

Segal A. (1984), *Finite Element Package SEPRAN*, Sepra analysis, Leidschendam, Holland.

Stahn D. and W. Döll (1978). Verfahren zum geradlinigen Schneiden von Flachglas mit Hilfe von thermisch induzierten Spannungen. *Deutsches Patentschrift 2813303*, applicant: Fraunhofer Institut, Germany

Stahn D., M. Schinker, W. Döll and E. Sommer (1980). Möglichkeiten zur Verbesserung von Bearbeitungsvorgängen an Glas auf Grund von Bruchuntersuchungen. *Glasstechnische Ber.* 53, 259-266

Stern M. (1979). Families of consistent conforming elements with singular derivative fields. *Int. J. Num. Meth. Eng.*, 14, 409-421.

Wilson W.K. and I.W. Yu (1979). The use of the J-integral in thermal stress crack problems. *Int. J. of Fracture*, 15, 377-387.